

# Morenci Groundwater Basin Profile



## Basin Summary Statistics

**Size<sup>1</sup>:** 1,599 square miles

**Elevation<sup>2</sup>:** Range: 3,268-10,722 ft; Median: 6,049 ft

**Top 3 land cover types by area<sup>3</sup>:** Evergreen Forest (52%), Shrub/Scrub (44%), Barren Land (1.4%)

**Major surface watershed(s)<sup>4</sup>:** San Francisco River, Upper Gila River

**Groundwater subbasins<sup>1</sup>:** None

**Groundwater-derived streamflow fraction<sup>5</sup>:**

**0.45** (Moderate)



Mean Annual Hydrologic Cycle Components (1980-2020)  
MORENCI

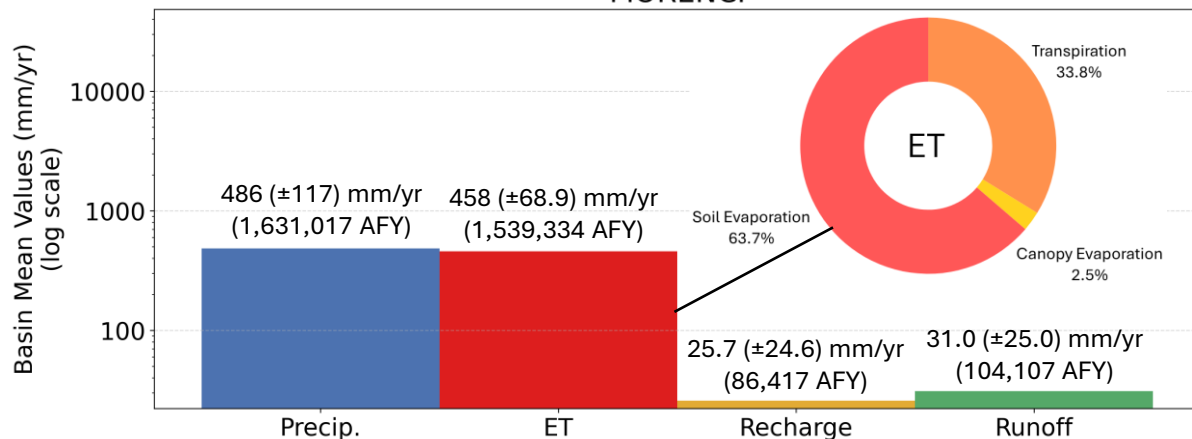


**Figure 1 (above).** Bar chart showing Noah-MP modeling results of the historical mean annual hydrologic cycle components (precipitation [P], evapotranspiration [ET], natural recharge, and runoff) in the basin from 1980-2020.<sup>6</sup> ET is partitioned into soil evaporation, canopy evaporation, and transpiration. It is possible for ET to be greater than P when there are other sources such as groundwater, surface water, or water in storage.

Mean Monthly Hydrologic Cycle Components (1980-2020)  
MORENCI

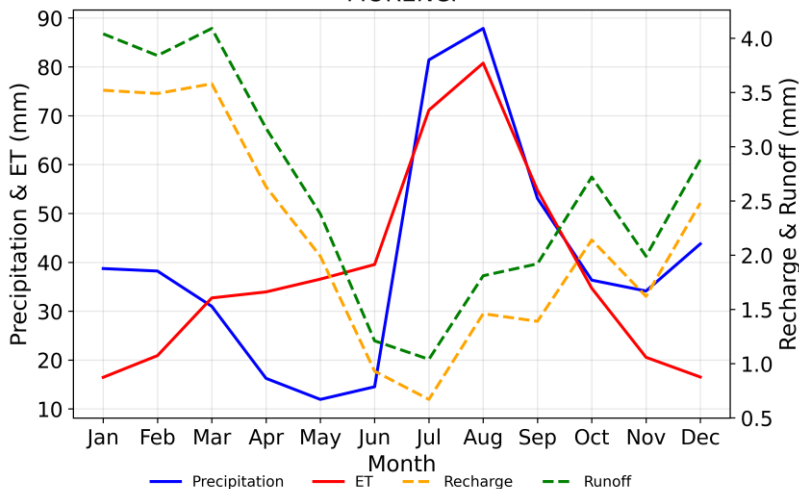


**Figure 2.** Graph showing monthly mean precipitation, ET, recharge, and runoff for the groundwater basin (1980-2020) from Noah-MP modeling results.<sup>6</sup>

Precipitation (P) in the Morenci basin is affected by the North American Monsoon during the summer months. The greatest atmospheric losses occur during the warmer months, where evapotranspiration (ET) exceeds P from mid-March through June and tracks with P from July to October. Soil evaporation makes up 63.7% of total ET in the basin, while transpiration comprises 33.8% and canopy evaporation accounts for the remainder (2.5%). Natural recharge (25.7 mm/yr) and runoff (31.0 mm/yr) peak from January to April due to springtime snowmelt and lower atmospheric demand. Groundwater supplies an estimated 45% of total streamflow in the Morenci basin.

# Morenci



**Figure 3 (below).** Gridded depiction of mean annual water fluxes across the groundwater basin from Noah-MP modeling (1980-2020): (a) precipitation, (b) evapotranspiration, (c) recharge, (d) runoff.<sup>6</sup> Major cities/towns<sup>7</sup> and Native American Reservation boundaries<sup>8</sup> are shown (as applicable) to help orient the reader.

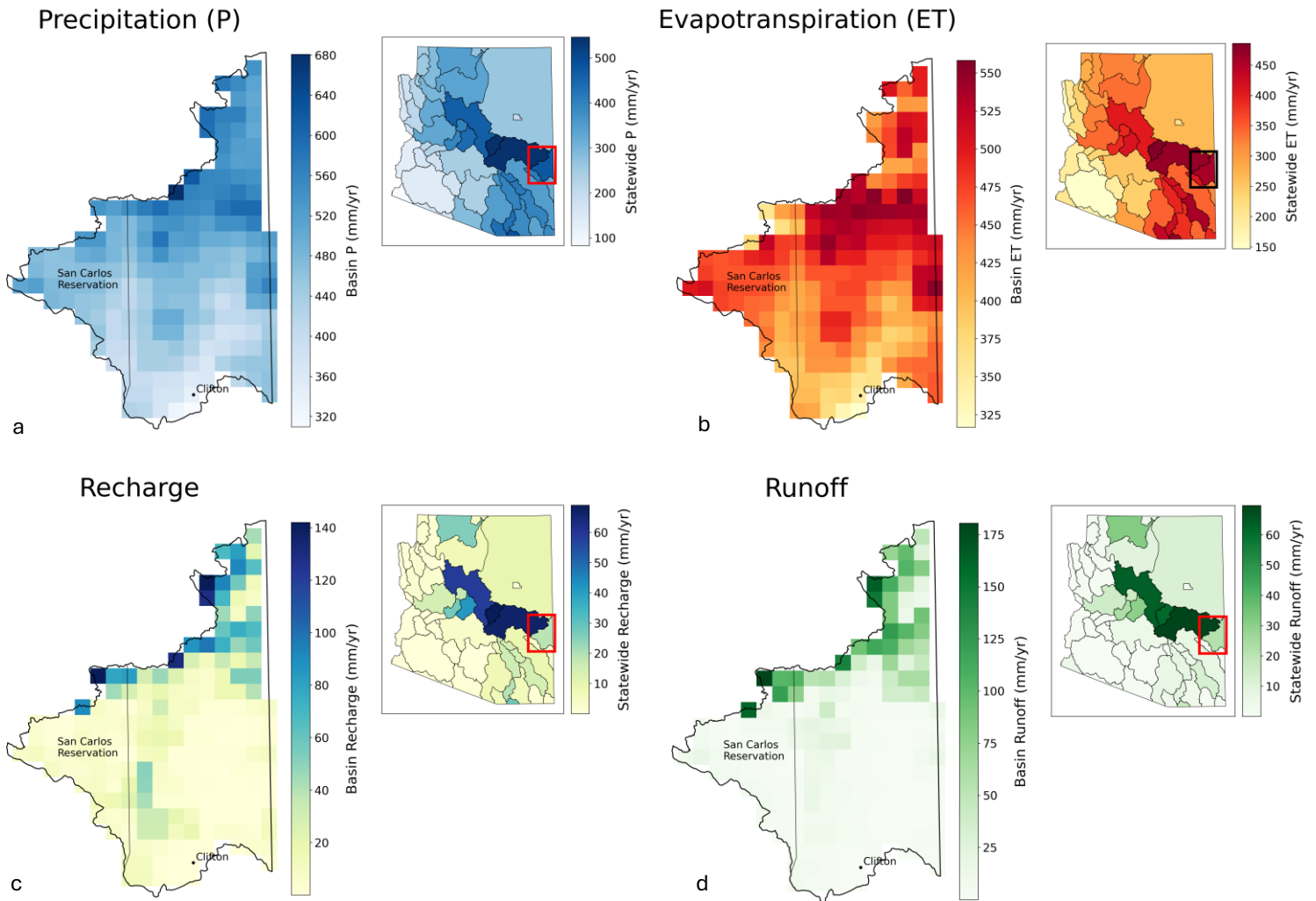
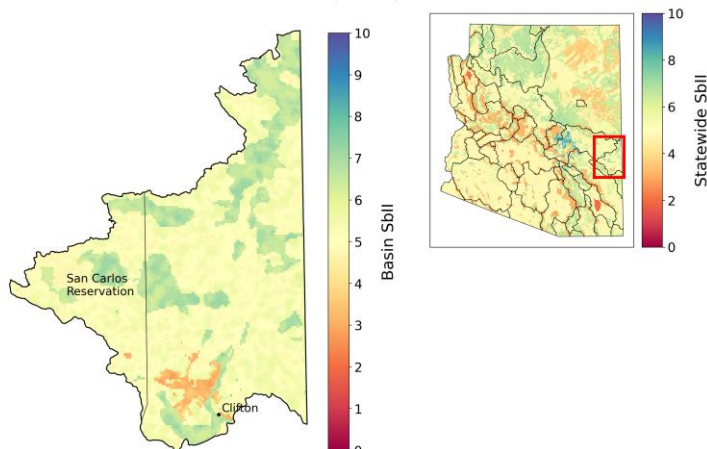


**Figure 4 (below).** Subsurface infiltration index (SbII) showing infiltration potential of the subsurface across the groundwater basin on a scale of 1-10 based on geologic features.<sup>9</sup>

## Subsurface Infiltration Index (SbII)



Precipitation (P) in the Morenci basin is greatest in the higher elevations in the northern portion of the basin, exceeding 640 mm/year on average. Evapotranspiration (ET, ~525 mm/yr), natural recharge (~120 mm/yr) and runoff (~150 mm/yr) are also highest in this region of the basin. The Morenci basin generally has moderate to high infiltration potential. The areas with highest infiltration potential result from deposits of rim gravels and weakly to moderately consolidated conglomerate that contains limestone.



## Climate Change Projections: Changes in Temperature, Precipitation, ET, Recharge, and Runoff (2060-2099 vs. 1981-2020)

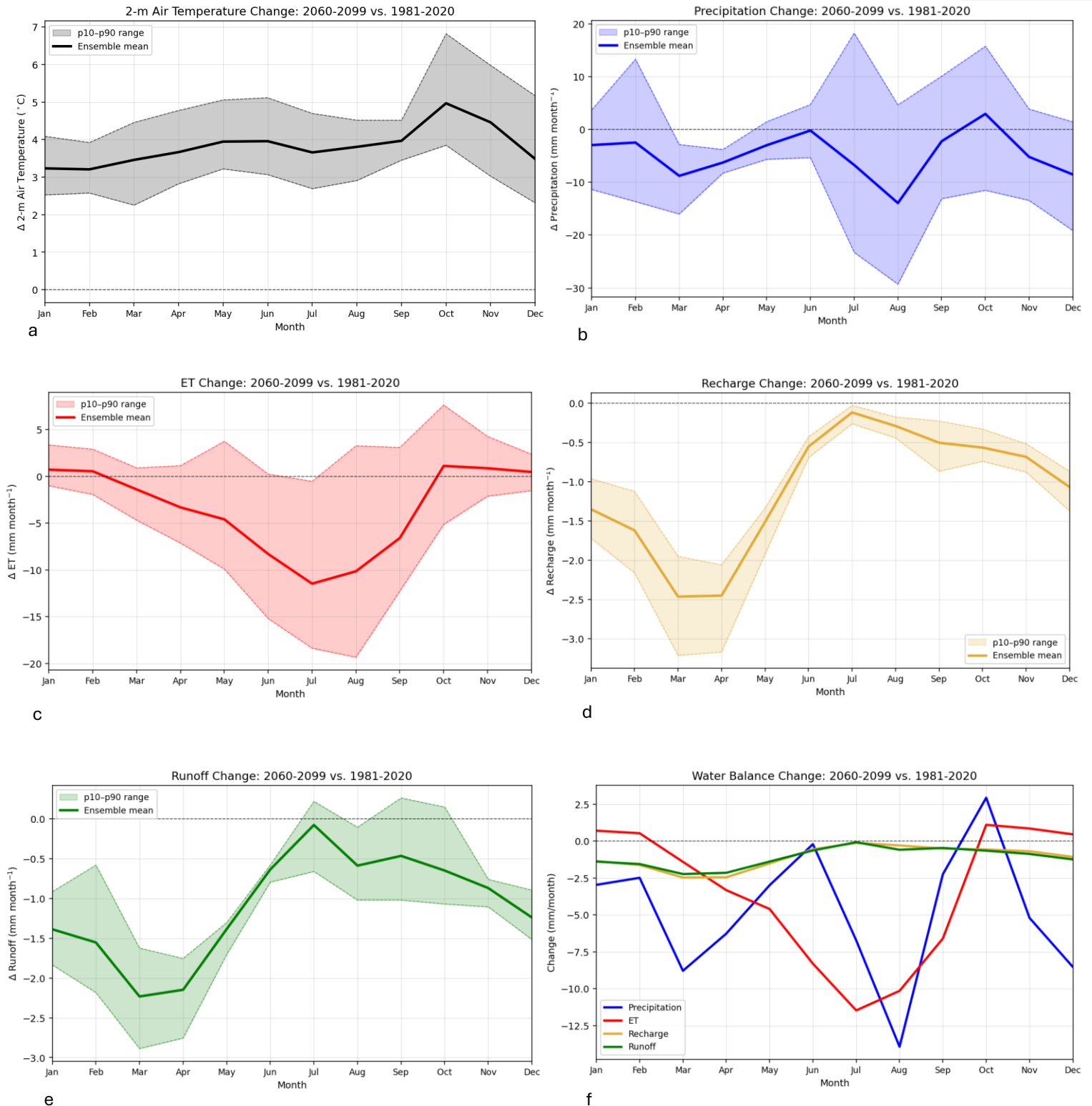


**Figure 5.** Plots (a)-(e) show projected changes in (a) temperature, (b) precipitation, (c) evapotranspiration (ET), (d) natural recharge, and (e) runoff statewide, comparing end of the 21<sup>st</sup> century to the historical record from 1981-2020 under the IPCC Scenario SSP3-7.0.<sup>10</sup> Plot (f) shows the change in the water balance components (P, ET, recharge, and runoff) on a single graph for direct comparison. The analysis uses 14 dynamically downscaled global climate models (GCM) at 9-km resolution and the Noah-MP land surface model. The ensemble mean of the 14 GCMs is shown in bold for each component of the hydrologic cycle, with the 10-90<sup>th</sup> percentile shaded to show model projection uncertainty.



Climate change projections across the Morenci basin show less precipitation throughout the majority of the year, with the exception of October, which shows an 8% (2.9 mm) increase in precipitation. The greatest declines in precipitation are projected for March-May (24-41% or -2.5 to -8.8 mm/month) and August (15% or -14 mm). Declines in natural recharge are projected for all months of the year, with projections in the highest recharge months (January-April) showing declines of 79-87% (-1.4 to -2.5 mm/month). Recharge projections are slightly negative (-0.06 to -0.16 mm/month) from July through November.\* Runoff is projected to decrease in all months of the year, with 72-84% (-1.4 to -2.3 mm/month) declines in the highest runoff months (January-April). Projected increases in temperature range from approximately 3.2 °C in February to 5.0 °C in October. Less water availability from precipitation in April-August leads to a projected 10-18% (-3.4 to -11 mm/month) decrease in evapotranspiration (ET) in those months compared to the baseline period.

\*Projected negative recharge values are attributed to increased capillary rise from the aquifer through the vadose zone due to climate factors, resulting in water loss from the system. Because the Noah-MP model does not include groundwater pumping, this indicates that climate-driven factors play a significant role in groundwater storage decline in Arizona.

### References

1. ADWR Groundwater Basin and Subbasin shapefiles. Retrieved from: <https://gisdata2016-11-18t150447874z-azwater.opendata.arcgis.com/>
2. USGS Digital Elevation Model data. Retrieved from: <https://apps.nationalmap.gov/downloader/>
3. Annual National Land Cover Database – Land Cover (2024). Retrieved from the Multi-Resolution Land Characteristics Consortium: <https://www.mrlc.gov/data>
4. USGS HUC8 Watersheds. Retrieved from: <https://hydro.nationalmap.gov/arcgis/rest/services/wbd/MapServer>
5. Mroczek, C., Springer, A. E., Gupta, N., Sankey, T., & Lucas, B. (2025). Regional base-flow index in arid landscapes using machine learning and instrumented records. *Journal of Hydrology: Regional Studies*, 62, 102778. <https://doi.org/10.1016/j.ejrh.2025.102778>
6. Gupta, A., Qiu, Y., Behrangi, A., & Niu, G. (2026). Noah-MP 40-Years Climatology for Water Balance over Ground Water Basins in Arizona, HydroShare, <http://www.hydroshare.org/resource/a3cc182071124849a463b6132213af23>. (Figures by Hinkley, M. & Mohsenzadeh Karimi, S.)
7. AZGeo City Points shapefile. Retrieved from AZGeo Data Hub: <https://azgeo-open-data-agic.hub.arcgis.com/datasets/azgeo::city-points/about>
8. Federal American Indian Reservation boundaries shapefile. Retrieved from: [https://services2.arcgis.com/FiaPA4ga0iQKduv3/arcgis/rest/services/Federal\\_American\\_Indian\\_Reservations\\_v1/FeatureServer](https://services2.arcgis.com/FiaPA4ga0iQKduv3/arcgis/rest/services/Federal_American_Indian_Reservations_v1/FeatureServer)
9. Lima, R., Springer, A., Sankey, T. (2026). Arizona Subsurface Infiltration Index v.2, HydroShare, <https://doi.org/10.4211/hs.abcd8aa1a793463ab33677ce9d46db58>
10. Qiu, Y. (2026). Future Projection of Hydroclimate over Arizona Version 2, HydroShare, <https://doi.org/10.4211/hs.a5751f0af305483682501f79d9af0bd7>

